



1
2
3
4
5
6
7
8
9
10
11
12
13
14
15
16
17
18
19
20
21
22
23
24

Effects of pan-Arctic snow cover and air temperature changes on soil heat content

Xiaogang Shi¹, Tara J. Troy² and Dennis P. Lettenmaier³

¹*CSIRO Land and Water, Canberra, Australian Capital Territory, Australia*

²*Department of Civil and Environmental Engineering, Lehigh University, Bethlehem, USA*

³*Department of Geography, University of California, Los Angeles, USA*

*Corresponding author:

Dennis P. Lettenmaier
Department of Geography
University of California, Los Angeles
dlettenm@ucla.edu
Phone: 310 794 4327



25 **Abstract**

26 Soil heat content (SHC) provides an estimate of the integrated effect of changes in the land
27 surface energy balance. It considers the specific heat capacity, soil temperature, and phase
28 changes of soil moisture as a function of depth. In contrast, soil temperature provides a much
29 more limited view of land surface energy flux changes. This is particularly important at high
30 latitudes, which have and are undergoing surface energy flux changes as a result of changes in
31 seasonal variations of snow cover extent (SCE) and hence surface albedo changes, among
32 other factors. Using the Variable Infiltration Capacity (VIC) land surface model forced with
33 gridded climate observations, we simulate spatial and temporal variations of SCE and SHC
34 over the pan-Arctic land region for the last half-century. On the basis of the SCE trends
35 derived from NOAA satellite observations in 5° latitude bands from April through June for
36 the period 1972-2006, we define a snow covered sensitivity zone (SCSZ), a snow covered
37 non-sensitivity zone (SCNZ), and a non-snow covered zone (NSCZ) for North America and
38 Eurasia. We then explore long-term trends in SHC, SCE, and surface air temperature (SAT)
39 and their corresponding correlations in NSCZ, SCSZ and SCNZ for both North America and
40 Eurasia. We find that snow cover downtrends have a significant impact on SHC changes in
41 SCSZ for North America and Eurasia from April through June. SHC changes in the SCSZ
42 over North America are dominated by downtrends in SCE rather than increasing SAT. Over
43 Eurasia, increasing SAT more strongly affects SHC than in North America. Overall,
44 increasing SAT during late spring and early summer is the dominant factor that has resulted in
45 SHC changes over the pan-Arctic domain, whereas reduced SCE plays a secondary role that is
46 only important in the SCSZ.

47 **Keywords:** pan-Arctic, snow cover extent, surface air temperature, soil heat content, Variable
48 Infiltration Capacity model, land surface energy budget



49 1. Introduction

50 Over the pan-Arctic land region, the rise in surface air temperature (SAT) in recent
51 decades has been almost twice as large as the global average (e.g., Serreze et al., 2000; Jones
52 and Moberg, 2003; Overland et al., 2004; Hinzman et al., 2005; White et al., 2007; Solomon et
53 al., 2007; Trenberth et al., 2007; Serreze et al., 2009; Screen and Simmonds, 2010; Cohen et al.,
54 2013; Walsh, 2014). Increases in SAT have been accompanied by increasing soil temperatures
55 with deeper active layer thickness across permafrost regions and decreasing frozen soil depths
56 in the seasonally frozen ground regions (e.g., Hinzman and Kane, 1992; Zhang et al., 2001;
57 Frauenfeld et al., 2004; Osterkamp, 2007; Qian et al., 2011; Smith et al., 2010, 2012;
58 Romanovsky et al., 2007, 2010, 2014; Streletskiy et al., 2015; Peng et al., 2016). Given the
59 potential for releases of soil carbon to the atmosphere at warmer ground temperatures, the land
60 surface warming at high latitudes has attracted considerable scientific attention (e.g., Stieglitz
61 et al., 2003; Zhang, 2005; Osterkamp, 2007; Heimann and Reichstein, 2008; Lawrence and
62 Slater, 2010; Frauenfeld and Zhang, 2011; Park et al., 2014; Kim et al., 2015; Yi et al., 2015).

63 Because snow is a strong insulator, it can limit the efficient transport of heat between
64 the atmosphere and the ground. Thus, snow plays an important role in determining how air
65 temperature signals propagate into and out of the soil column (Gold, 1963; Goodrich, 1982;
66 Osterkamp and Romanovsky, 1996; Stieglitz et al., 2003; Mann and Schmidt, 2003; Zhang,
67 2005; Bartlett et al., 2005; Iwata et al., 2008; Lawrence and Slater, 2010; Park et al., 2015). In
68 general, seasonal snow cover results in relatively higher mean annual ground temperatures,
69 especially at high latitudes where stable snow cover lasts from a few weeks to several months



70 (Zhang, 2005; Frauenfeld and Zhang, 2011). In recent decades, a substantial retreat of snow
71 cover extent (SCE) has been observed during late spring and early summer (Groisman et al.,
72 1994; Déry and Brown, 2007; Brown et al., 2010; Derksen and Brown, 2012; Shi et al., 2011,
73 2013) in the visible satellite imagery produced by the National Oceanic and Atmospheric
74 Administration (NOAA) (Robinson et al., 1993; Frei and Robinson, 1999). Moreover, these
75 negative SCE trends are well reproduced by simulations using the Variable Infiltration
76 Capacity (VIC) land surface model (Liang et al., 1994; Cherkauer and Lettenmaier, 1999) for
77 both North America and Eurasia (Shi et al., 2011, 2013).

78 Over the past decades, observed soil temperatures across the pan-Arctic domain have
79 been used as an indicator of climate change (e.g., Osterkamp and Romanovsky, 1999; Zhang et
80 al., 2001; Frauenfeld et al., 2004; Smith et al., 2004; Beltrami et al., 2006; Romanovsky et al.,
81 2002, 2007; Frauenfeld and Zhang, 2011). Recent studies have also attempted to explain the
82 impact of changing seasonal snow cover and air temperature on the ground thermal regime
83 over the pan-Arctic by using soil temperature as an index (e.g., Zhang et al., 1997; Zhang and
84 Stamnes, 1998; Romanovsky et al., 2002; Bartlett et al., 2004, 2005; Lawrence and Slater,
85 2010; Park et al., 2015). However, *in situ* soil temperatures are problematic because some
86 important physical processes are basically neglected, such as the change in mass due to soil
87 moisture changes and the latent heat effects of freezing and thawing. These effects can be
88 important at high latitudes with seasonally and permanently frozen soils and result in the
89 complicated interpretation for the effects of seasonal snow cover and air temperature on the
90 ground thermal regime.



91 To provide a more complete understanding of the effects of high latitude land surface
92 warming, we used an alternative approach based on soil heat content (SHC) as an indicator of
93 changes in the ground thermal regime, which can provide an integrated measure that accounts
94 for changes in temperature, moisture, and latent heat effects. SHC has been used in various
95 studies to document how the land surface responds to atmospheric changes (e.g., Levitus et al.,
96 2001, 2005; Beltrami et al., 2002, 2006; Hu and Feng, 2004; Hansen et al., 2005; Mottaghy and
97 Rath, 2006; Troy, 2010).

98 We explore here the effects of downtrends in SCE and increases in SAT on SHC over
99 the pan-Arctic land region, with particular emphasis on trends and variability during the late
100 spring and early summer seasons. In Section 2, we describe the observations and model-
101 derived data sets on which our analyses are based. In Section 3, we define three study zones
102 and the computation of SHC. In Section 4, we evaluate the model results, explore trends in
103 SHC, and examine correlations between SCE, SAT, and SHC and the relative roles of snow
104 cover downtrends and increasing SAT on SHC changes. We summarize our findings in Section
105 5.

106 **2. Data sets**

107 **2.1. Observed SCE and SAT data**

108 As described in Shi et al. (2013), we used observed monthly values of SCE, which were
109 extracted from the weekly snow cover extent for the Northern Hemisphere maintained at the
110 National Snow and Ice Data Center (NSIDC). These data span the period October 1966
111 through June 2014 (Brodzik and Armstrong, 2013), with a spatial resolution of 25 km. We



112 restricted our period of analysis to begin in 1972 because some charts between 1967 and 1971
113 are missing (Robinson, 2000). The data set has become a widely used tool for deriving trends
114 in climate-related studies (Groisman et al., 1994; Déry and Brown, 2007; Flanner et al., 2009;
115 Derksen et al., 2010; Derksen and Brown, 2011, 2012; Shi et al., 2011, 2013), notwithstanding
116 uncertainties in some parts of the domain for certain times of the year, such as summertime
117 over northern Canada (Wang et al., 2005). Monthly SAT anomaly data were taken from the
118 Climatic Research Unit (CRU, Brohan et al., 2006), and are based on anomalies from the long-
119 term mean temperature for the period 1961-1990 for each month since 1850. The land-based
120 monthly data are on a regular 0.5° by 0.5° global grid. We regrid these data, including the
121 NOAA SCE observations that were aggregated from the 25 km product, to the 100 km EASE
122 grid using an inverse distance interpolation as implemented in Shi et al. (2013).

123 **2.2. Modeled SHC from VIC**

124 The version of VIC used for this study is 4.1.2, which includes some updates to the
125 model's algorithms for cold land processes. For instance, the model includes a snow
126 parameterization that represents snow accumulation and ablation processes using a two-layer
127 energy and mass balance approach (Andreadis et al., 2009), a canopy snow interception
128 algorithm when an overstory is present (Storck et al., 2002), a finite-difference frozen soils
129 algorithm (Cherkauer and Lettenmaier, 1999) with sub-grid frost variability (Cherkauer and
130 Lettenmaier, 2003), and an algorithm for the sublimation and redistribution of blowing snow
131 (Bowling et al., 2004), as well as a lakes and wetlands model (Bowling and Lettenmaier, 2010).



132 The snow parameterization in VIC represents snow accumulation and ablation
133 processes using a two-layer energy and mass balance approach (Andreadis et al. 2009) and a
134 canopy snow interception algorithm (Storck et al. 2002) when an overstory is present. In the
135 VIC model setup for this study, each grid cell was partitioned into five elevation (snow) bands,
136 which can include multiple land cover types. The snow model was applied to each grid cell and
137 elevation band separately. When snow water equivalent is greater than a threshold, the model
138 assumes that snow fully covers that elevation band. For each grid cell, the simulated SCE is
139 calculated as the average over the elevation bands. The current version of the frozen soils
140 algorithm uses a finite difference solution in the algorithm that dates to the work of Cherkauer
141 and Lettenmaier (1999). To improve spring peak flow predictions, a parameterization of the
142 spatial distribution of soil frost was developed (Cherkauer and Lettenmaier, 2003). Adam
143 (2007) described some significant modifications to the frozen soils algorithm, including the
144 bottom boundary specification using the observed soil temperature datasets of Zhang et al.
145 (2001), the exponential thermal node distribution, the implicit solver using the Newton-
146 Raphson method, and an excess ground ice and ground subsidence algorithm in VIC 4.1.2.

147 To model permafrost properly, our implementation used a depth of 15 m with 18 soil
148 thermal nodes (STN) exponentially distributed with depth and a no flux bottom boundary
149 condition (Jennifer Adam, personal communication). When the no flux bottom boundary
150 condition is selected for the soil column, the VIC model solves the ground heat fluxes using the
151 finite difference method. This means that the soil temperature at the bottom boundary can
152 change, but there is no loss or gain of heat energy through the boundary. Compared to the
153 constant heat flux (e.g., Neumann) boundary condition, the no flux bottom boundary condition



154 method adds slightly to the computation time, but is especially useful for very long simulations
155 in climate change studies and permafrost simulations.

156 We used the same study domain as documented in Shi et al. (2013), which is defined as
157 all land areas draining into the Arctic Ocean, as well as those regions draining into the Hudson
158 Bay, Hudson Strait, and the Bering Strait, but excluding Greenland (because its snow cover is
159 mainly perennial in nature). The model simulations used calibrated parameters, such as soil
160 depths and infiltration characteristics, from Su et al. (2005). The VIC runs are at a three-hour
161 time step in full energy balance mode (meaning that the model closes a full surface energy
162 budget by iterating for the effective surface temperature, as contrasted with water balance
163 mode, in which the surface temperature is assumed to equal the surface air temperature). The
164 model is driven by daily precipitation, maximum and minimum temperatures, and wind speed
165 at a spatial resolution (EASE grid) of 100 km. Also, VIC has an internal algorithm to estimate
166 the incoming shortwave and longwave radiation fluxes that are based on location and
167 meteorological conditions and implicitly used to force the model. The forcing data were
168 constructed from 1948 through 2006 using methods outlined by Adam and Lettenmaier (2008),
169 as described in Shi et al. (2013). To set up the right initial conditions in VIC, especially for the
170 thermal state, we initialized the model with a 100-year climatology created by randomly
171 sampling years from the 1948-1969 meteorological forcings. Also, we calculated the
172 correlation coefficients between SCE, SAT, and SHC using the 35-year time series spatially
173 averaged for the three zones over North America and Eurasia along the 15 m soil profile.
174 Through the above processes, the effects due to the propagation of SAT signals to the deeper
175 soil depth become weak. After validating the VIC simulation, we reconstructed SHC from



176 1970 to 2006 for the pan-Arctic land area.

177 **3. Methodology**

178 **3.1. Definition of study zones**

179 The NOAA weekly SCE data (hereafter SCE) were analyzed to determine whether or
180 not there are regions with significant changes of SCE in North America and Eurasia. Figure 1(a)
181 shows the spatial distribution of long-term monthly means of SCE from April through June for
182 the 35-year period over North American and Eurasian pan-Arctic domains. Figures 1 (b) and (c)
183 illustrate the latitudinal variations of SCE trends and their area fractions over the North
184 American and Eurasian study domains from April through June. The percentage under each bar
185 chart is the trend significance expressed as a confidence level for each 5° of latitude, while the
186 solid line shows the latitudinal patterns in the snow cover area fractions for each month, which
187 in general are at a minimum for the lowest latitude band, and then increase with latitude
188 poleward.

189 Based on the latitudinal changes of NOAA SCE as shown in Figure 1, we identified
190 different study zones for North America and Eurasia. From April through June, snow mostly
191 covers latitude bands north of 45°N over the pan-Arctic land area, which are denoted as snow
192 covered zones (SCZs) in Figure 1. The rest of the study domains were denoted as non-snow
193 covered zones (NSCZs) (see Figure 1(a) for North America and Eurasia, respectively). Within
194 the SCZs, we selected only those latitudinal bands within which SCE trends were statistically
195 significant for further analyses. For each month, we denoted these bands as snow cover
196 sensitivity zones (SCSZs). For the remaining bands in the SCZs, there is no significant snow



197 cover downtrends, and these bands are defined as snow covered non-sensitivity zones (SCNZs).
198 In Figures 1(b) and 1(c), we use different gray-shaded arrows to highlight the North American
199 and Eurasian SCZs, which include the SCSZs and SCNZs. For example, the SCSZ for May in
200 North America has six latitude bands from 45-50°N to 70-75°N, whereas there is only one
201 band (45-50°N) for the Eurasian SCSZ in April. Given the large-scale snow cover in Eurasia
202 and North America, the effects caused by the differences in snow depth can be neglected.

203 3.2. Definition of SHC for the soil thermal nodes

204 SHC, also called soil enthalpy in the literature, is a measure of the heat stored in the soil
205 column. It has been applied in many previous studies (e.g., Hu and Feng, 2004; Hansen et al.,
206 2005; Levitus et al., 2005; Beltrami et al., 2006; Mottaghy and Rath, 2006; Troy, 2010). At its
207 simplest, it is written as a vertical integral as in Hu and Feng (2004):

$$H = \int_0^z C_s T(z) dz \quad (1)$$

208
209 where H is the soil heat content, C_s is the specific heat capacity, and $T(z)$ is the soil temperature
210 as a function of depth z . This formulation neglects two important physical processes that are
211 important at high latitudes. First, the change in mass due to soil moisture (both liquid and
212 frozen) changes, which changes the heat energy stored in the soil column, is not included.
213 Second, the latent heat effects of freezing and thawing are neglected. These effects can be
214 important at high latitudes with seasonally and permanently frozen soils. Consequently, we
215 calculated the SHC changes as follows for each STN (n):

$$H_n = \int (C_s f_s \rho_s + C_l f_l \rho_l + C_i f_i \rho_i) dT - \int L_f df_i \quad (2)$$

216



217 where H_n is the SHC value at node n , C is the specific heat capacity of soil, liquid water and
218 frozen water (subscripts s , l , and i , respectively), f is the fraction of soil and liquid and frozen
219 water, ρ is density, dT is the change in temperature, and L_f is the latent heat of fusion. We
220 neglect the heat content of air in the soil pores. We computed the change in SHC was
221 calculated for each model time step, accounting for changes in the fraction of liquid and frozen
222 water with each time step. The fraction of soil remains constant in time. This is essentially the
223 same formulation as Mottaghy and Rath (2006) with the addition of the heat capacity of the
224 soil matrix included. To calculate the total change in SHC for the soil column, the vertical
225 integral was calculated accounting for the spacing of the nodes. Therefore, the total change of
226 SHC is an integrated value over a soil thermal profile from the surface to a specified depth z ,
227 rather than an average value for the specific layer. The calculation process for the SHC change
228 is consistent with our motivation here, which is to investigate the impacts of snow cover and
229 air temperature changes on SHC as a function of soil depth.

230 As described in Section 2.2, we used a depth of 15 m with 18 STNs in the VIC
231 implementation. To maximize computational efficiency, the spacing of soil thermal nodes in
232 the frozen soils framework in VIC should reflect the variability in soil temperature (Adam,
233 2007). Because the greatest variability in soil temperature occurs near the surface, it is
234 preferable to have tighter node spacing near the surface and wider node spacing near the
235 bottom boundary where temperature variability is reduced. Therefore, these 18 STNs were
236 distributed exponentially with depth as indicated in Table 1. The SHC for each STN in the soil
237 column was calculated for each model time step (three hours) and then aggregated for each
238 month from April through June. Along the soil profile from the top to the bottom, the first STN



239 was named as STN0 with a depth of 0 m indicating it is at the surface, while the deepest one is
240 STN17 with a soil depth of 15 m. The SHC for STN17 represents an integrated thermal value
241 for the soil profile. To simplify the analyses, we calculated SHC changes relative to 1970,
242 using the start of our historical VIC runs as our datum. All monthly SHC values are relative to
243 this datum and as such represent the change in SHC since January 1, 1970. In addition, we
244 calculated monthly SHC anomalies on the basis of monthly means averaged over each NSCZ,
245 SCSZ and SCNZ of North America and Eurasia by removing the 1981-1990 mean. Figure 2
246 shows the area percentages of NSCZ, SCSZ, and SCNZ in North America and Eurasia from
247 April through June for the period 1972-2006. The experimental design for assessing the effects
248 of pan-Arctic snow cover and air temperature changes on SHC in NSCZ, SCSZ, and SCNZ
249 over North America and Eurasia from April through June for the period 1972-2006 is shown in
250 Figure 3. For example, we can isolate the impact of increasing SAT on SHC changes in NSCZ,
251 which has no presence of snow. Within SCSZ, the effects of both SCE and SAT changes on
252 SHC can be compared. Moreover, we can investigate the effect of snow cover changes by
253 comparing SCSZ and SCNZ, as there are snow cover downtrends in SCSZ whereas none is in
254 SCNZ.

255 **3.3. Mann-Kendall trend test**

256 To analyze long-term changes in the monthly time series of SCE, SAT and SHC over
257 the North America and Eurasia study zones, we used the non-parametric Mann-Kendall (MK)
258 trend test (Mann, 1945; Kendall, 1975), a rank-based method applicable for trend significance.
259 In addition, we used the Sen slope estimator (Sen, 1968) to estimate trend slopes. The MK
260 trend test has been applied in many previous studies for identifying trends in meteorological



261 and hydrologic variables (e.g., Lettenmaier et al., 1994; Zhang et al., 2001; Burn et al., 2004;
262 Déry and Brown, 2007; Shi et al., 2011, 2013), and has been found to perform well. We used a
263 5% significance level (two-sided test).

264 **3.4. Pearson's product-moment correlation coefficient**

265 We used the Pearson's product-moment correlation coefficient was used to assess
266 relationships and computed it separately for each study zone from April through June. Given
267 the 35-year record, correlations are statistically significant at a level of $p < 0.025$ (two-sided
268 test) when the absolute value of the sample correlation is greater than 0.34 based on the
269 Student t-test with 33 degrees of freedom. Through correlation analyses, it is possible to
270 identify the relative roles of downtrends in SCE and increasing SAT on pan-Arctic SHC
271 changes.

272 **4. Results**

273 **4.1. Model validation**

274 There are no unified temperature data sets that fully cover our study domain. Here we
275 used a monthly historical soil temperature dataset, which is available across the former Soviet
276 Union, with the earliest observation beginning in 1882 and the last in 1990 (Zhang et al., 2001).
277 Soil temperature was measured at various depths between 0.2 and 3.2 meters, with the largest
278 number of measurements at 0.2, 0.8, 1.6, and 3.2 meters. The temporal coverage varies by
279 station, with some stations only having a few years of data and others with decades of
280 continuous measurements (Troy, 2010). Because there are gaps in the observational data, the
281 VIC results were screened to only include a grid cell when the corresponding station had data.



282 In this study, we compared soil temperature predicted by VIC against historical soil
283 temperature observations at 146 stations across the former Soviet Union as shown in Figure
284 4(a). When calculating the annual mean, a year was only included in the analysis if data existed
285 for all twelve months. To compare across the region, we calculated the annual soil temperature
286 anomaly at 0.2, 0.8, 1.6, and 3.2 meters for these 146 stations across the former Soviet Union,
287 which is confined to the common period of 1970-1990 between VIC and observations.

288 Figure 4(b) compares modeled and observed soil temperature anomalies to evaluate the
289 ability of the model to replicate observed trends. The results reveal that the model slightly
290 underestimates the trend in temperature but captures the interannual variability of the soil
291 temperature dynamics, which are similar to Troy (2010). In addition, Figure 4(b) also shows
292 the correlation coefficients between modeled and observed time series for the period from 1970
293 to 1990. The significance level is based on a two-tailed Student's *t* test with 19 degrees of
294 freedom. The VIC and observed soil temperature time series at 0.2, 0.8, 1.6, and 3.2 meters are
295 highly correlated (two-sided $p < 0.01$). Therefore, we conclude that VIC is able to reproduce
296 soil temperature profiles and provides a surrogate for scarce observations for estimation of
297 long-term changes in SHC at high latitudes.

298 **4.2. SCE and SAT trends**

299 The MK trend tests were performed on the monthly time series of SCE and SAT area-
300 averaged over the North America and Eurasia study zones. Tables 2 and 3 summarize the SCE
301 and SAT trends and their significance levels in NSCZ, SCSZ, and SCNZ for both continents
302 from April through June for the entire study period (1972-2006). Table 2 shows that



303 statistically significant ($p < 0.025$) negative trends were detected in SCE for both North
304 American and Eurasian SCSZs, as found in many previous studies. In SCNZ, the decreasing
305 trends in SCE are all non-significant, and the absolute values of trend slopes are much smaller
306 than that in SCSZ. As reported in Table 3, increasing SAT trends were detected for both
307 continents except for North America in May. For June in North America and for May and June
308 in Eurasia, these SAT trends are statistically significant in NSCZ, SCSZ, and SCNZ. In SCNZ,
309 increasing SAT trends are all statistically significant for both continents except for Eurasia in
310 April.

311 Based on the above long-term trends in SCE and SAT for NSCZ, SCSZ, and SCNZ, it
312 is clear that the impact of increasing SAT on SHC changes can be isolated in NSCZ as there is
313 no presence of snow. In SCSZ, the effects of both SCE and SAT changes on SHC can be
314 compared as indicated in Figure 3. By comparing SCSZ and SCNZ, we can investigate the
315 effect of snow cover changes on SHC changes, as there are snow cover downtrends in SCSZ
316 whereas SCE is not a factor in SCNZ. Figure 2 shows the area percentages for NSCZ, SCSZ
317 and SCNZ in North America and Eurasia from April through June. In Eurasia, the SCNZ
318 dominates in April as there is no significant snow cover change for most portions of the study
319 domain. When snow cover retreats, the SCSZ and NSCZ in Eurasia expands significantly in
320 May and June. Over North America, the SCE retreat occurs earlier than in Eurasia. Especially
321 for May, most regions in North America have snow cover downtrends. In June, Figure 2
322 clearly illustrates that SCE is already gone for most portions of Eurasia.

323 **4.3. SHC trends**



324 Figure 5 shows the trends and significance levels of the VIC-derived SHC for each
325 STN in NSCZ, SCSZ and SCNZ over North America and Eurasia from April through June.
326 Figures 5a and 5b show that there are obvious differences for trends and significance levels
327 between North America and Eurasia. For North America (Figure 5a), the SHC in SCSZ
328 increases significantly from the top thermal nodes to the deeper ones, whereas in NSCZ and
329 SCNZ, most thermal nodes have increasing trends, which are not statistically significant. Over
330 Eurasia, this is quite different. In Figure 5b, almost all the thermal nodes in NSCZ, SCSZ, and
331 SCNZ over Eurasia from April through June show statistically significant increasing trends in
332 SHC, indicating that there are different effects of downtrends in SCE and increasing SAT on
333 SHC changes between Eurasia and North America.

334 **4.4. Effects of SCE and SAT changes on SHC**

335 To identify the relative roles of decreasing SCE and increasing SAT on pan-Arctic SHC
336 changes, we examined the correlations among SHC, SCE, and SAT over NSCZ, SCSZ and
337 SCNZ for both North America and Eurasia. Figure 6 shows correlations between observed
338 SCE and VIC-derived SHC in NSCZ, SCSZ, and SCNZ over North America and Eurasia from
339 April through June. In SCSZ, the correlations between SCE and SHC are all statistically
340 significant over both continents from April through June. Over SCNZ, however, the
341 correlations are much smaller and are not statistically significant. These results imply that the
342 static snow cover insulation in SCNZ does not significantly impact SHC changes over the pan-
343 Arctic. Additionally, no correlation exists between SHC and SCE in NSCZ. Furthermore, the
344 implied impact of snow cover extent changes on SHC is similar for North America and Eurasia.



345 Figure 7 shows correlations between observed SAT and simulated SHC monthly time
346 series in NSCZ, SCSZ, and SCNZ over North America and Eurasia from April through June.
347 Overall, the results indicate that SAT has a statistically significant impact on SHC changes in
348 NSCZ. Moreover, SAT has greater influence on SHC over Eurasia than in North America as
349 shown in Figure 7. All the correlations over Eurasia are statistically significant except for
350 SCSZ and SCNZ in April, for which the increasing trends in SAT are not statistically
351 significant.

352 The correlations described in Figures 6 and 7 were calculated on the time series of
353 variables using the Pearson's product-moment method. Both the effects of secular trend and
354 variability are included. We separated these two components and explored the relative roles of
355 the linear trend and the variability (detrended) in the corresponding correlations. Table 4
356 summarizes correlation coefficients due to the linear trend and the variability between SHC
357 derived from VIC and SCE observations in SCSZ and SCNZ over North America and Eurasia
358 for the period 1972-2006. The significance level (*p*-value) was calculated using a two-tailed
359 Student *t*-test with 33 degrees of freedom. Basically, SHC and SCE in NSCZ, SCSZ, and
360 SCNZ are highly correlated due to the secular trend, except for May and June in SCNZ over
361 North America, where the SCE trends are zero. In contrast, the variability components are
362 small and not statistically significant. Clearly, the relationships between SHC and SCE time
363 series are mainly dominated by snow cover changes in each study zone over North America
364 and Eurasia. We also applied the same analyses for the VIC-derived SHC and CRU SAT, as
365 reported in Table 5. The linear trends in SAT dominate the correlations between SHC derived
366 from VIC and CRU SAT in NSCZ, SCSZ, and SCNZ over North America and Eurasia. In



367 contrast, the effect of SAT variability is weak and not statistically significant. Therefore, the
368 relationships between the SHC and SAT time series as shown in Figure 7 are mainly due to
369 increasing SAT in each study zone over North America and Eurasia.

370 As described above, SHC changes are significantly affected by downtrends in SCE and
371 increasing SAT from April through June over North America and Eurasia for the period 1972-
372 2006. But the variability in SCE and SAT have insignificant effects on SHC. Comparing the
373 correlations in Figures 6 and 7 suggests that: (1) downtrends in SCE have a significant impact
374 on SHC changes in SCSZ, which is similar for both continents; (2) over North America, SHC
375 changes in SCSZ during late spring and early summer are dominated by snow cover
376 downtrends rather than increasing SAT; (3) over Eurasia, increasing SAT more strongly affects
377 SHC than in North America; and (4) overall, increasing SAT has the dominant influence on
378 SHC for North America and Eurasia, and reduced SCE plays a secondary role that is only
379 important in SCSZ.

380 **5. Discussion and Conclusions**

381 We defined three study zones (NSCZ, SCSZ, and SCNZ) within the North American
382 and Eurasian portions of the pan-Arctic land area based on observed SCE trends. Using these
383 definitions of zones, we focused on the effects of pan-Arctic snow cover and air temperature
384 changes on SHC by exploring long-term trends in SHC, SCE, and SAT and their
385 corresponding correlations in NSCZ, SCSZ, and SCNZ for North America and Eurasia. We
386 find that North American and Eurasian late spring and early summer (from April through June)
387 SHC has increasing trends for the period 1972-2006. However, there are obvious differences



388 between North America and Eurasia as to the magnitudes of SHC trend slopes and significance
389 levels. For North America, SHC in SCSZ has mostly increased significantly, whereas in NSCZ
390 and SCNZ, most thermal nodes show non-significant increasing trends. For Eurasia, almost all
391 the thermal nodes in NSCZ, SCSZ, and SCNZ have statistically significant increasing trends,
392 indicating that there are different effects of snow cover downtrends and increasing SAT on
393 SHC changes between North America and Eurasia. By analyzing the corresponding
394 correlations, we conclude that snow cover downtrends have a significant impact on SHC
395 changes in SCSZ for North America and Eurasia from April through June. SHC changes in
396 SCSZ over North America are dominated by snow cover downtrends rather than increasing
397 SAT. Over Eurasia, increasing SAT more strongly affects SHC than in North America. Overall,
398 increasing SAT during late spring and early summer has the dominant influence on SHC
399 changes over the pan-Arctic, and reduced SCE plays a secondary role that is only important in
400 SCSZ.

401 In this article, we mainly focused on the impacts of snow cover and air temperature
402 changes on SHC for the temporal scale. The value of SHC is that it estimates the heat stored in
403 the soil column by considering the specific heat capacity and soil temperature as a function of
404 depth. In the calculation, the specific heat capacity of soil, liquid water and frozen water were
405 included, as well as the latent heat of fusion, rather than soil temperature alone. Therefore, it
406 provides an estimate of the integrated changes in heat content for the vertical soil column,
407 whereas soil temperature only gives point measurements at specific depths. Given that soil
408 temperature can sit at the freezing point while soil freeze/thaw is going on, this also gives a
409 better integrative estimate of the heat budget. It would be interesting to investigate the spatial



410 distribution of SHC trends across the pan-Arctic domain in our future work. In addition, we
411 formulated our estimate (Equation 2) to be based on SCE instead of snow depth due to the
412 following reasons. First, both snow depth and SCE can affect the amount of energy absorbed
413 by the ground, but they are at different levels. Snow depth affects the insulating properties of
414 the snowpack, whereas changes in SCE (whether or not snow is present) have a first order
415 effect on the amount of energy absorbed by the ground and hence the rate of soil warming (e.g.,
416 Euskirchen et al., 2007), owing to the large difference in the amount of downward solar
417 radiation absorbed by snow covered land as contrasted with snow free land, particularly in
418 spring (e.g., Déry and Brown, 2007). Second, trends in snow depth over the pan-Arctic domain
419 are highly heterogeneous (Dyer and Mote, 2006; Park et al., 2012, Yi et al., 2015), whereas
420 SCE trends have been much more coherent on a regional basis (Brown and Mote, 2009). For
421 this reason, the decreasing trends in SCE have a dominant impact on the SHC trends, while
422 trends in snow depth are comparatively minor. Therefore, the big SHC changes are associated
423 with transitions from snow cover to snow free in the spring, when downward solar radiation is
424 increasing rapidly.

425 In the 1970s, global warming first became evident beyond the bounds of natural
426 variability, but increases in global mean surface temperatures have stalled in the 2000s. This
427 pause is commonly called the “hiatus.” We know that Earth's climate system is accumulating
428 excess solar energy owing to the build-up of greenhouse gases in the atmosphere. However,
429 global mean surface temperatures fluctuate much more than these can account for. Therefore,
430 the energy imbalance is manifested not just as surface atmospheric and ground warming, but



431 also as melting sea and land ice and heating of the oceans. Especially, more than 90% of the
432 heat goes into the oceans (Trenberth and Fasullo, 2013).

433 Notwithstanding that the primary focus of this work is on technical issues associated
434 with trends in high latitude moisture and energy fluxes, the work has broader implications that
435 deserve mention. The importance of snow to high latitude energy fluxes, especially as a result
436 of strong contrasts between the albedo of snow covered and snow free surfaces and hence the
437 potential for positive climate impacts as the high latitudes warm, is well known. Furthermore,
438 the low thermal conductivity of snow insulates the ground, and resultant contrasts in the snow
439 surface temperature as contrasted with bare ground affect the transfer of heat to and from the
440 atmosphere (Barry et al., 2007). These factors can influence the climate not only of high
441 latitude regions, but also, via teleconnections, of lower latitudes. More directly, changes in
442 snow cover patterns have major effects on water availability, industry, agriculture, and
443 infrastructure and affect the livelihoods of the inhabitants of high latitude land regions.
444 Furthermore, certain industries depend heavily on snow cover and frozen soils. Oil and gas
445 companies, for example, use ice roads in the Arctic to gain access to resource fields, and are
446 negatively impacted by permafrost changes. Another impact of snow cover changes is
447 increased heat storage in frozen soils, which ultimately results in permafrost thawing. Thawing
448 permafrost already has affected the stability of infrastructure over parts of the pan-Arctic
449 domain, such as buildings, roads, railways, and pipelines (Osterkamp and Romanovsky, 1999).
450 In addition, the northern high latitudes contain about twice as much carbon as the global
451 atmosphere, largely stored in permafrost and seasonally thawed soil active layers (Hugelius et
452 al., 2014). The rising soil heat content may affect future soil carbon releases with potential



453 feedback on climate change (Schuur et al., 2015). Furthermore, permafrost degradation in
454 many high latitude regions is of concern for hydrological processes (Romanovsky et al., 2010;
455 Watts et al., 2012) and for changes in vegetation composition and establishment (Tape et al.,
456 2006; Sturm et al., 2005; Shi et al., 2015). All of these potential impacts are related to the
457 interaction of air, snow and soil freeze-thaw processes, and point to the importance of work
458 like that reported herein in a broader context.



459 **Acknowledgements**

460 This work was supported by NASA grants NNX07AR18G and NNX08AU68G to the
461 University of Washington. The authors thank former colleagues Professor Jennifer Adam
462 (Washington State University), and Dr. Ted Bohn (Arizona State University) for their
463 assistance and comments.

464



465 **References**

466 Adam, J. C.: Understanding the causes of streamflow changes in the Eurasian Arctic, Ph.D.
467 thesis, 174 pp., University of Washington, Seattle, WA, 2007.

468 Adam, J. C. and Lettenmaier, D. P.: Application of new precipitation and reconstructed
469 streamflow products to streamflow trend attribution in northern Eurasia. *J. Clim.*, *21*,
470 1807-1828, 2008.

471 Andreadis, K. M., Storck, P., and Lettenmaier, D. P.: Modeling snow accumulation and
472 ablation processes in forested environments, *Water Resour. Res.*, *45*, W05429,
473 doi:10.1029/2008WR007042, 2009.

474 Barry, R. G., Armstrong, R., Callaghan, T., Cherry, J., Gearheard, S., Nolin, A., Russell, D.,
475 and Zaeckler, C.: *Chapter 4: Snow. In Global outlook for ice and snow*, ed. United
476 Nations Environment Programme, 39-62, Hertfordshire, England, 2007.

477 Bartlett, M. G., Chapman, D. S., and Harris, R. N.: Snow and the ground temperature record of
478 climate change, *J. Geophys. Res.*, *109*, F04008, doi:10.1029/2004JF000224, 2004.

479 Bartlett, M. G., Chapman, D. S., and Harris, R. N.: Snow effect on North American ground
480 temperatures, 1950-2002, *J. Geophys. Res.*, *110*, F03008, doi:10.1029/2005JF000293,
481 2005.

482 Beltrami, H., Smerdon, J., Pollack, H. N., and Huang, S.: Continental heat gain in the global
483 climate system, *Geophys. Res. Lett.*, *29*(8), 1167, doi:10.1029/2001GL014310, 2002.

484 Beltrami, H., Bourlon, E., Kellman, L., and González-Rouco, J. F.: Spatial patterns of ground



- 485 heat gain in the Northern Hemisphere, *Geophys. Res. Lett.*, *33*, L06717,
486 doi:10.1029/2006GL025676, 2006.
- 487 Bowling, L. C. and Lettenmaier, D. P.: Modeling the effects of lakes and wetlands on the water
488 balance of arctic environments, *J. Hydrometeorol.*, *11*(2), 276-295, 2010.
- 489 Bowling, L. C., Pomeroy, J. W., and Lettenmaier, D. P.: Parameterization of blowing-snow
490 sublimation in a macroscale hydrology model, *J. Hydrometeorol.*, *5*, 745-762, 2004.
- 491 Brodzik, M. and Armstrong R.: Northern Hemisphere EASE-Grid 2.0 Weekly Snow Cover and
492 Sea Ice Extent, Version 4, Boulder, Colorado USA, NASA National Snow and Ice Data
493 Center Distributed Active Archive Center, 2013.
- 494 Brohan, P., Kennedy, J., Harris, I., Tett, S., and Jones, P.: Uncertainty estimates in regional and
495 global observed temperature changes: A new dataset from 1850, *J. Geophys. Res.*, *111*,
496 D12106, 2006.
- 497 Brown, R. D. and Robinson, D. A.: Northern Hemisphere spring snow cover variability and
498 change over 1922–2010 including an assessment of uncertainty, *The Cryosphere*, *5*,
499 219-229, 2011.
- 500 Brown, R. D., Derksen, C., and Wang, L.: A multi-data set analysis of variability and change in
501 Arctic spring snow cover extent, 1967-2008, *J. Geophys. Res.*, *115*, D16111, 2010.
- 502 Brown, R. D. and Mote, P. W.: The response of Northern Hemisphere snow cover to a
503 changing climate, *J. Climate*, *22*, 2124-2145, 2009.
- 504



- 505 Cherkauer, K. A. and Lettenmaier, D. P.: Hydrologic effects of frozen soils in the upper
506 Mississippi River basin, *J. Geophys. Res.*, *104*, 19599-19610, 1999.
- 507 Cherkauer, K. A. and Lettenmaier, D. P.: Simulation of spatial variability in snow and frozen
508 soil, *J. Geophys. Res.*, *108*, 8858, 2003.
- 509 Cohen, J., Furtado, J. C., Barlow, M. A., Alexeev, V. A., and Cherry, J. C.: Arctic warming,
510 increasing snow cover and widespread boreal winter cooling, *Environ. Res. Lett.*, *7*,
511 014007, 1-8, 2013.
- 512 Déry, S. J. and Brown, R. D.: Recent Northern Hemisphere snow cover extent trends and
513 implications for the snow-albedo feedback, *Geophys. Res. Lett.*, *34*, L22504, doi:
514 10.1029/2007GL031474, 2007.
- 515 Derksen, C. and Brown, R. D.: Terrestrial snow (Arctic) in state of the climate in 2010, *Bull.*
516 *Am. Meteorol. Soc.*, *92*, S154-S155, 2011.
- 517 Derksen, C. and Brown, R. D.: Spring snow cover extent reductions in the 2008-2012 period
518 exceeding climate model projections, *Geophys. Res. Lett.*, *39*, L19504, 2012.
- 519 Derksen, C. and Wang, L.: Terrestrial snow (Arctic) in state of the climate in 2009, *Bull. Am.*
520 *Meteorol. Soc.*, *91*, S93-S94, 2010.
- 521 Dyer, J. L. and Mote, T. L.: Spatial variability and trends in observed snow depth over North
522 America, *Geophys. Res. Lett.*, *33*, L16503, 2006.
- 523 Euskirchen, E. S., McGuire, A. D., and Chapin, F. S.: Energy feedbacks of northern high-
524 latitude ecosystems to the climate system due to reduced snow cover during 20th
525 century warming, *Glob. Change Biol.*, *13*, 2425-2438, 2007.



- 526 Flanner, M., Zender, C., Hess, P., Mahowald, N., Painter, T., Ramanathan, V., and Rasch, P.:
527 Springtime warming and reduced snow cover from carbonaceous particles, *Atmos.*
528 *Chem. Phys.*, *9*, 2481-2497, 2009.
- 529 Frauenfeld, O. W., Zhang, T., Barry, R. G., and Gilichinsky, D.: Interdecadal changes in
530 seasonal freeze and thaw depths in Russia, *J. Geophys. Res.*, *109*, D05101,
531 doi:10.1029/2003JD004245, 2004.
- 532 Frauenfeld, O. W. and Zhang, T.: An observational 71-year history of seasonally frozen ground
533 changes in the eurasian high latitudes, *Environ. Res. Lett.*, *6*, 044024, 2011.
- 534 Frei, A. and Robinson, D. A.: Northern Hemisphere snow extent: Regional variability 1972-
535 1994, *Int. J. Climatol.*, *19*, 1535-1560, 1999.
- 536 Gold, L. W.: Influence of snow cover on the average annual ground temperature at Ottawa,
537 Canada, *IAHS Publ.*, *61*, 82-91, 1963.
- 538 Goodrich, L. E.: The influence of snow cover on the ground thermal regime, *Canadian*
539 *Geotechnical J.*, *24*, 160-163, 1982.
- 540 Groisman, P. Y., Karl, T. R., Knight, R. W., and Stenchikov, G. L.: Changes of snow cover,
541 temperature, and radiative heat balance over the Northern Hemisphere, *J. Clim.*, *7*,
542 1633-1656, 1994.
- 543 Hansen, J., et al.: Earth's energy imbalance: Confirmation and implications, *Science*, *308*,
544 1431-1435, 2005.
- 545 Hinzman, L. D. and Kane, D. L.: Potential response of an Arctic watershed during a period of



- 546 global warming, *J. Geophys. Res.*, 97, 2811-2820, 1992.
- 547 Heimann, M. and Reichstein, M.: Terrestrial ecosystem carbon dynamics and climate
548 feedbacks, *Nature*, 451(7176), 289-292, 2008.
- 549 Hinzman, L. D., and Coauthors: Evidence and implications of recent climate change in
550 northern Alaska and other arctic regions, *Clim. Change*, 72, 251-298, 2005.
- 551 Hu, Q. and Feng, S.: A Role of the Soil Enthalpy in Land Memory, *J. Climate*, 17, 3633-3643,
552 2004.
- 553 Hugelius, G., and Coauthors: Estimated stocks of circumpolar permafrost carbon with
554 quantified uncertainty ranges and identified data gaps, *Biogeosciences*, 11, 6573-6593,
555 2014.
- 556 Iwata, Y., Hayashi, M., and Hirota, T.: Effects of snow cover on soil heat flux and freeze-thaw
557 processes, *J. Agric. Meteorol.*, 64, 301-308, 2008.
- 558 Jones, P. D. and Moberg, A.: Hemispheric and large-scale surface air temperature variations:
559 An extensive revision and an update to 2001, *J. Clim.*, 16, 206-223, 2003.
- 560 Kim, Y., Kimball, J. S., Robinson, D. A., and Derksen, C.: New satellite climate data records
561 indicate strong coupling between recent frozen season changes and snow cover over
562 high northern latitudes, *Environ. Res. Lett.*, 10, 084004, 2015.
- 563 Lawrence, D. M. and Slater, A. G.: The contribution of snow condition trends to future ground
564 climate, *Clim. Dyn.*, 34, 969-981, 2010.
- 565 Levitus, S., Antonov, J., and Boyer, T.: Warming of the world ocean, 1955-2003, *Geophys. Res.*



- 566 *Let.*, 32, L02604, 2005.
- 567 Levitus, S., Antonov, J., Wang, J., Delworth, T. L., Dixon, K., and Broccoli, A.:
568 Anthropogenic warming of the Earth's climate system, *Science*, 292, 267-270, 2001.
- 569 Liang, X., Lettenmaier, D. P., Wood, E., and Burges, S.: A simple hydrologically based model
570 of land surface water and energy fluxes for general circulation models, *J. Geophys. Res.*,
571 99, D17, 14415-14428, 1994.
- 572 Mann, H. B.: Nonparametric tests against trend, *J. Econom. Sci.*, 245-259, 1945.
- 573 Mann, M. E. and Schmidt, G. A.: Ground vs. surface air temperature trends: Implications for
574 borehole surface temperature reconstructions, *Geophys. Res. Lett.*, 30, 1607, 2003.
- 575 Mottaghy, D. and Rath, V.: Latent heat effects in subsurface heat transport modeling and their
576 impact on palaeotemperature reconstructions, *Geophys. J. Int.*, 164, 236-245, 2006.
- 577 Osterkamp, T. E. and Romanovsky, V. E.: Characteristics of changing permafrost temperatures
578 in the Alaskan Arctic, U.S.A., *Arct. Alp. Res.*, 28(3), 267-273, 1996.
- 579 Osterkamp, T. E. and Romanovsky, V. E.: Evidence for warming and thawing of discontinuous
580 permafrost in Alaska, *Permafr. Periglac. Process.*, 10(1), 17-37, 1999.
- 581 Osterkamp, T. E.: Characteristics of the recent warming of permafrost in Alaska, *J. Geophys.*
582 *Res.* 112, F02S02, 2007.
- 583 Overland, J. E., Spillane, M. C., Percival, D. B., Wang, M. Y., and Mofjeld, H. O.: Seasonal
584 and regional variation of pan-Arctic surface air temperature over the instrumental
585 record, *J. Clim.*, 17, 3263-3282, 2004.



- 586 Park, H., Yabuki H., and Ohata T.: Analysis of satellite and model datasets for variability and
587 trends in Arctic snow extent and depth, 1948-2006, *Polar Sci.*, 2012.
- 588 Park, H., Sherstiukov, A. B., Fedorov, A. N., Polyakov, I. V., and Walsh, J. E.: An observation
589 based assessment of the influences of air temperature and snow depth on soil
590 temperature in Russia, *Environ. Res. Lett.*, 9, 064026, 2014.
- 591 Park, H., Fedorov, A. N., Zheleznyak, M. N., Konstantinov, P. Y., and Walsh, J. E.: Effect of
592 snow cover on pan-Arctic permafrost thermal regimes, *Clim. Dyn.* 44 2873-95, 2015.
- 593 Peng, S., Ciais, P., Krinner, G., Wang, T., Gouttevin, I., McGuire, A. D., Lawrence, D., Burke,
594 E., Chen, X., Decharme, B., Koven, C., MacDougall, A., Rinke, A., Saito, K., Zhang,
595 W., Alkama, R., Bohn, T. J., Delire, C., Hajima, T., Ji, D., Lettenmaier, D. P., Miller, P.
596 A., Moore, J. C., Smith, B., and Sueyoshi, T.: Simulated high-latitude soil thermal
597 dynamics during the past 4 decades, *The Cryosphere*, 10, 179-192, doi:10.5194/tc-10-
598 179-2016, 2016.
- 599 Qian, B., Gregorich, E. G., Gameda, S., Hopkins, D. W., and Wang, X. L.: Observed soil
600 temperature trends associated with climate change in Canada, *J. Geophys. Res.*, 116,
601 D02106., 2011.
- 602 Robinson, D. A.: Weekly Northern Hemisphere snow maps: 1966-1999, Preprints, *12th Conf.*
603 *on Applied Climatology*, Asheville, NC, Amer. Meteor. Soc., 12-15, 2000.
- 604 Robinson, D. A., Dewey, K. F., and Heim, Jr R. R.: Global snow cover monitoring: An update,
605 *Bull. Amer. Meteor. Soc.*, 74, 1689-1696, 1993.



- 606 Romanovsky, V., Smith, S., Yoshikawa, K., and Brown, J.: Permafrost temperature records:
607 indicators of climate change, *EOS, Transactions of AGU*, 83, 589-594, 2002.
- 608 Romanovsky, V. E., Sazonova, T. S., Balobaev, V. T., Shender, N. I., and Sergueev, D. O.:
609 Past and recent changes in air and permafrost temperatures in eastern Siberia, *Global*
610 *Planet. Change*, 56, 399-413, 2007.
- 611 Romanovsky, V. E., Smith, S. L., and Christiansen, H. H.: Permafrost thermal state in the polar
612 Northern Hemisphere during the international polar year 2007-2009: a synthesis,
613 *Permafrost Periglac.*, 21, 106-116, 2010.
- 614 Romanovsky, V. E. and Coauthors: Terrestrial permafrost (in 'state of the climate in 2013')
615 *Bull. Am. Meteorol. Soc.*, 95, S139-141, 2014.
- 616 Schuur, E. A. G., and Coauthors: Climate change and the permafrost carbon feedback, *Nature*,
617 520, 171-179, 2015.
- 618 Sturm, M., and Coauthors: Winter biological processes could help convert arctic tundra to
619 shrubland, *BioScience*, 55, 17-26, 2005.
- 620 Screen, J. A. and Simmonds, I.: The central role of diminishing sea ice in recent Arctic
621 temperature amplification, *Nature*, 464, 1334-1337, 2010.
- 622 Sen, P. K.: Estimates of the regression coefficient based on Kendall's tau, *J. Am. Stat. Assoc.*,
623 1379-1389, 1968.
- 624 Serreze, M., and Coauthors: Observational evidence of recent change in the northern high-
625 latitude environment, *Clim. Change*, 46, 159-207, 2000.



- 626 Serreze M. C., Barrett, A. P., Stroeve, J. C., Knidig, D. N., and Holland, M. M.: The
627 emergence of surface-based Arctic amplification, *The Cryosphere*, 3, 11-9, 2009.
- 628 Shi, X., Groisman, P. Y., Déry, S. J., and Lettenmaier, D. P.: The role of surface energy fluxes
629 in pan-Arctic snow cover changes, *Environ. Res. Lett.*, 6, 035204, 2011.
- 630 Shi, X., Déry, S. J., Groisman, P. Y., and Lettenmaier, D. P.: Relationships between recent
631 pan-Arctic snow cover and hydroclimate trends, *J. Clim.*, 26, 2048-2064, 2013.
- 632 Shi, X., Marsh, P., and Yang, D.: Warming spring air temperatures, but delayed spring
633 streamflow in an Arctic headwater basin, *Environ. Res. Lett.*, 10(6), 064003, 2015.
- 634 Smith, N. V., Saatchi, S. S., and Randerson, J. T.: Trends in high northern latitude soil freeze
635 and thaw cycle from 1988 to 2002, *J. Geophys. Res.*, 109, D12101, 2004.
- 636 Smith, S. L., Romanovsky, V. E., Lewkowitz, A. G., Burn, C. R., Allard, M., Clow, G. D.,
637 Yoshikawa, K., and Throop, J.: Thermal state of permafrost in North America: a
638 contribution to the international polar year, *Permafrost Periglac.*, 21, 117-135, 2010.
- 639 Smith, S. L., Throop, J., and Lewkowitz, A. G.: Recent changes in climate and permafrost
640 temperatures at forested and polar desert sites in northern Canada, *Can. J. Earth Sci.*,
641 49, 914-924, 2012.
- 642 Solomon, S., Qin, D., Manning, M., Marquis, M., Averyt, K., Tignor, M. M. B., Miller, H. L.
643 Jr., and Chen Z., Eds.: *Clim. Change 2007: The Physical Science Basis*, Cambridge
644 University Press, 996 pp, 2007.
- 645 Stieglitz, M., Déry, S. J., Romanovsky, V. E., and Osterkamp, T. E.: The role of snow cover in



- 646 the warming of arctic permafrost, *Geophys. Res. Lett.*, 30, 1721, doi:
647 10.1029/2003GL017337, 2003.
- 648 Storck, P., Lettenmaier, D. P., and Bolton, S. M.: Measurement of snow interception and
649 canopy effects on snow accumulation and melt in a mountainous maritime climate,
650 Oregon, United States, *Water Resour. Res.*, 38, 1223, 2002.
- 651 Streletskiy, D. A., Sherstukov, A. B., Nelson, F. E., Frauenfeld, O. W.: Changes in the 1963-
652 2013 shallow ground thermal regime in Russian permafrost regions, *Environ. Res. Lett.*,
653 10, 125005, 2015.
- 654 Su, F., Adam, J. C., Bowling, L. C., and Lettenmaier, D. P.: Streamflow simulations of the
655 terrestrial Arctic domain, *J. Geophys. Res.*, 110, 0148-0227, 2005.
- 656 Tape, K., Sturm, M., and Racine, C.: The evidence for shrub expansion in Northern Alaska and
657 the Pan-Arctic, *Glob. Change Biol.*, 12, 686-702, 2006.
- 658 Trenberth, K. E., and Coauthors: Observations: Surface and atmospheric climate change, in
659 *Climate Change 2007: The Physical Science Basis, contribution of working group I to*
660 *the fourth assessment report of the intergovernmental panel on climate change*, edited
661 by S. Solomon et al., 235-336, Cambridge Univ. Press, New York, 2007.
- 662 Trenberth, K. E. and Fasullo J. T.: An apparent hiatus in global warming? *Earth's Future*, 1,
663 19-32, 2013.
- 664 Troy, T. J.: The hydrology of northern Eurasia: uncertainty and change in the terrestrial water
665 and energy budgets, Ph.D. thesis, 164 pp., Princeton University, Princeton, NJ, 2010.



- 666 Walsh, J. E.: Intensified warming of the Arctic: causes and impacts on middle latitudes, *Glob.*
667 *Planet. Change*, 117, 52-63, 2014.
- 668 Wang, L., Sharp, M., Brown, R., Derksen, C., and Rivard, B.: Evaluation of spring snow
669 covered area depletion in the Canadian Arctic from NOAA snow charts, *Remote Sens.*
670 *Environ.*, 95, 453-463, 2005.
- 671 Watts, J. D., Kimball, J. S., Jones, L. A., Schroeder, R., and McDonald, K. C.: Satellite
672 Microwave remote sensing of contrasting surface water inundation changes within the
673 Arctic–Boreal Region, *Remote Sens. Environ.*, 127, 223-236, 2012.
- 674 White, D., and Coauthors: The arctic freshwater system: changes and impacts, *J. Geophys. Res.*,
675 112, G04S54, 2007.
- 676 Wiesnet, D., Ropelewski, C., Kukla, G., and Robinson, D.: A discussion of the accuracy of
677 NOAA satellite-derived global seasonal snow cover measurements, Proc. Vancouver
678 Symp.: Large Scale Effects of Seasonal Snow Cover, Vancouver, BC, Canada, *IAHS*
679 *Publ. 166*, 291-304, 1987.
- 680 Yi, Y., Kimball, J. S., Rawlins, M. A., Moghaddam, M., and Euskirchen, E. S.: The role of
681 snow cover affecting boreal-arctic soil freeze–thaw and carbon dynamics,
682 *Biogeosciences*, 12, 5811-5829, 2015.
- 683 Zhang, T.: Influence of the seasonal snow cover on the ground thermal regime: An overview,
684 *Rev. Geophys.*, 43, RG4002, 2005.
- 685 Zhang, T. and Stamnes, K.: Impact of climatic factors on the active layer and permafrost at



686 Barrow, Alaska, *Permafrost. Periglac. Process.*, 9, 229-246, 1998.

687 Zhang, T., Osterkamp, T. E., and Stamnes, K.: Effects of climate on the active layer and
688 permafrost on the North Slope of Alaska, U.S.A., *Permafrost. Periglac. Process.*, 8, 45-67,
689 1997.

690 Zhang, T., Barry, R. G., Gilichinsky, D., Bykhovets, S. S., Sorokovikov, V. A., and Ye, J. P.:
691 An amplified signal of climatic change in soil temperatures during the last century at
692 Irkutsk, Russia, *Clim. Change*, 49, 41-76, 2001.

693



List of Figures

694 **Figure 1.** (a) Spatial distribution of monthly mean snow cover extent (SCE) from NOAA
695 satellite observations (OBS) over North America and Eurasia in the pan-Arctic land region
696 (non-snow covered zone (NSCZ) and snow covered zone (SCZ)) for April (top panel), May
697 (middle panel), and June (bottom panel) for the period 1972-2006. The SCE trends in 5° (N)
698 latitude bands and their area fractions over (b) North American and (c) Eurasian SCZ,
699 including the snow covered sensitivity zone (SCSZ) and snow covered non-sensitivity zones
700 (SCNZ) as indicated by the arrows. The percentage under each bar chart is the trend
701 significance for each 5° (N) of latitude (expressed as a confidence level).

702 **Figure 2.** Area percentages of NSCZ, SCSZ, and SCNZ in North America and Eurasia from
703 April through June for the period 1972-2006.

704 **Figure 3.** Experimental design for assessing the effects of pan-Arctic snow cover and air
705 temperature changes on soil heat content (SHC) in NSCZ, SCSZ, and SCNZ over North
706 America and Eurasia from April through June for the period 1972-2006.

707 **Figure 4.** (a) Geographical distribution of 146 observation sites for soil temperature across the
708 former Soviet Union. The color bar at right indicates the number of archived years of data
709 ending in 1990. (b) Comparisons between observed and modeled soil temperature anomalies
710 averaged over 146 observation sites across the former Soviet Union for the period of 1970-
711 1990 at the depths of 0.2 m, 0.8 m, 1.6 m, and 3.2 m, respectively. The correlation is
712 statistically significant at a level of $p < 0.025$.

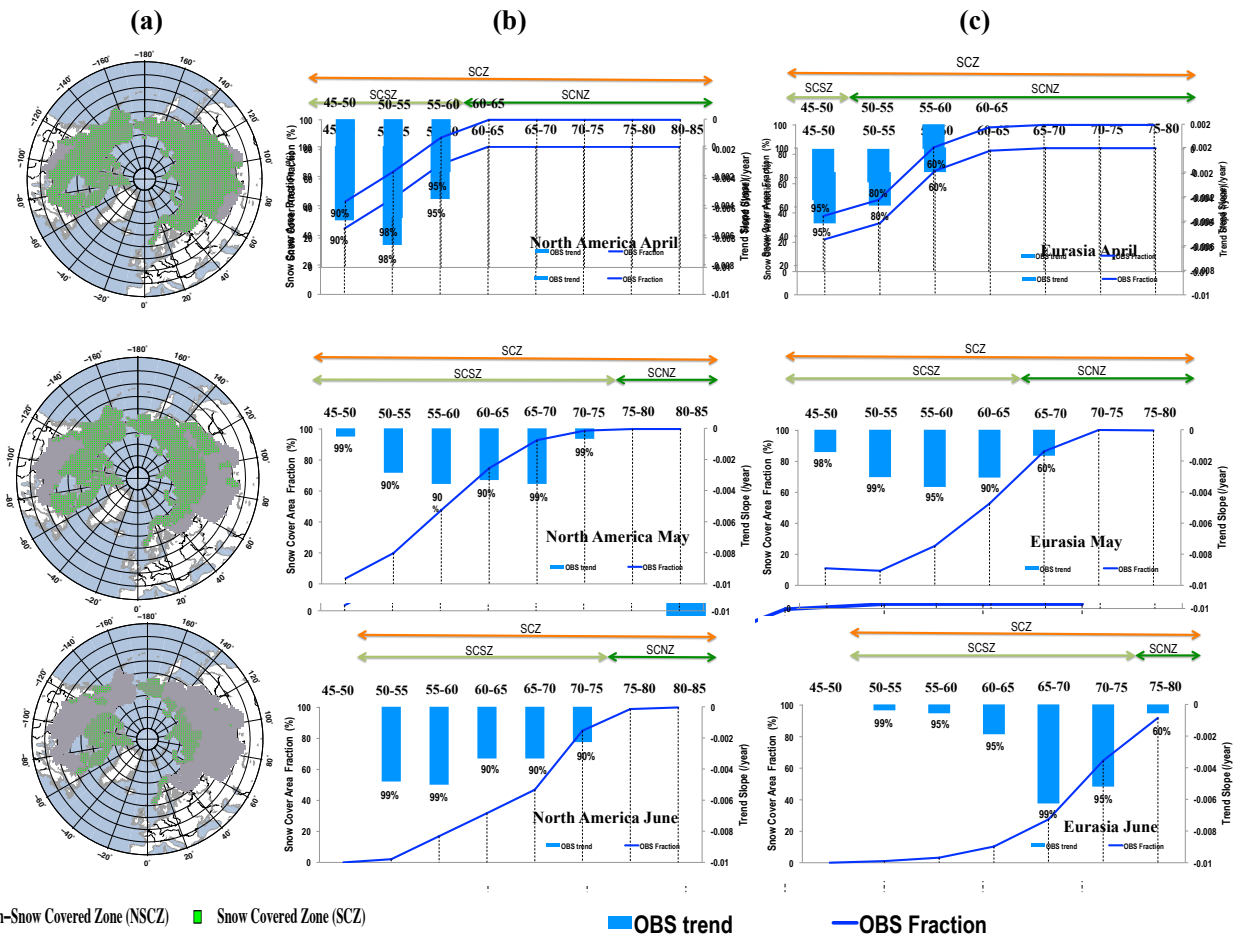
713 **Figure 5.** Trend analyses for SHC at the depth of each soil thermal node derived from the
714 VIC model in NSCZ, SCSZ, and SCNZ over (a) North America and (b) Eurasia from April



715 through June for the period 1972-2006. The significance level (expressed as a confidence
716 level) was calculated using a two-sided Mann-Kendall trend test. Trend slope units are MJm^{-2}
717 year^{-1} .

718 **Figure 6.** Correlations between NOAA SCE and simulated SHC in NSCZ, SCSZ, and SCNZ
719 over North America and Eurasia from April through June for the period 1972-2006. The
720 correlation with asterisks is statistically significant at a level of $p < 0.025$ when its absolute
721 value is greater than 0.34.

722 **Figure 7.** Correlations between observed SAT and simulated SHC in NSCZ, SCSZ and SCNZ
723 over North America and Eurasia from April through June for the period 1972-2006. The
724 correlation with asterisks is statistically significant at a level of $p < 0.025$ when its absolute
725 value is greater than 0.34.



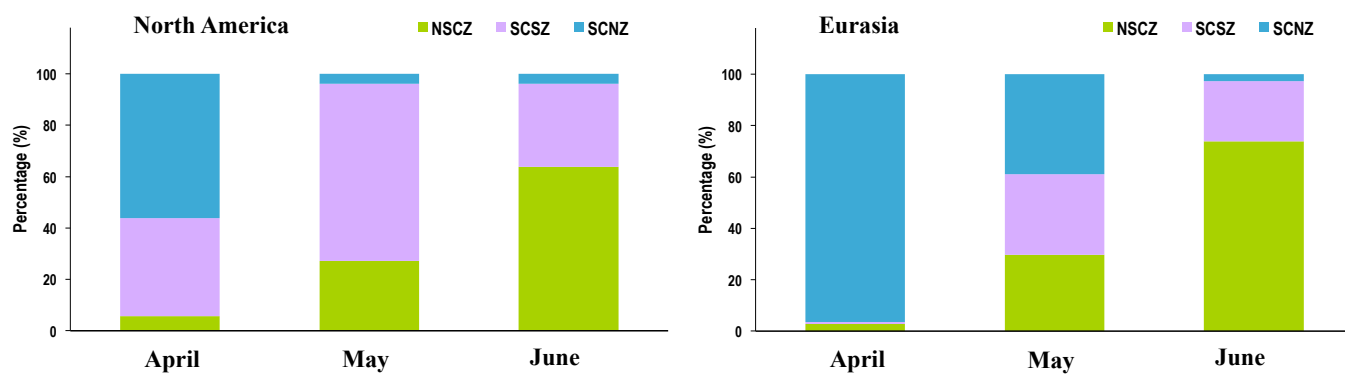


27 **Figure 1.** (a) Spatial distribution of monthly mean snow cover extent (SCE) from NOAA satellite observations (OBS) over North America and
28 Eurasia in the pan-Arctic land region (non-snow covered zone (NSCZ) and snow covered zone (SCZ)) for April (top panel), May (middle
29 panel), and June (bottom panel) for the period 1972-2006. The SCE trends in 5° (N) latitude bands and their area fractions over (b) North
30 American and (c) Eurasian SCZ, including the snow covered sensitivity zone (SCSZ) and snow covered non-sensitivity zones (SCNZ) as
31 indicated by the arrows. The percentage under each bar chart is the trend significance for each 5° (N) of latitude (expressed as a confidence
32 level).



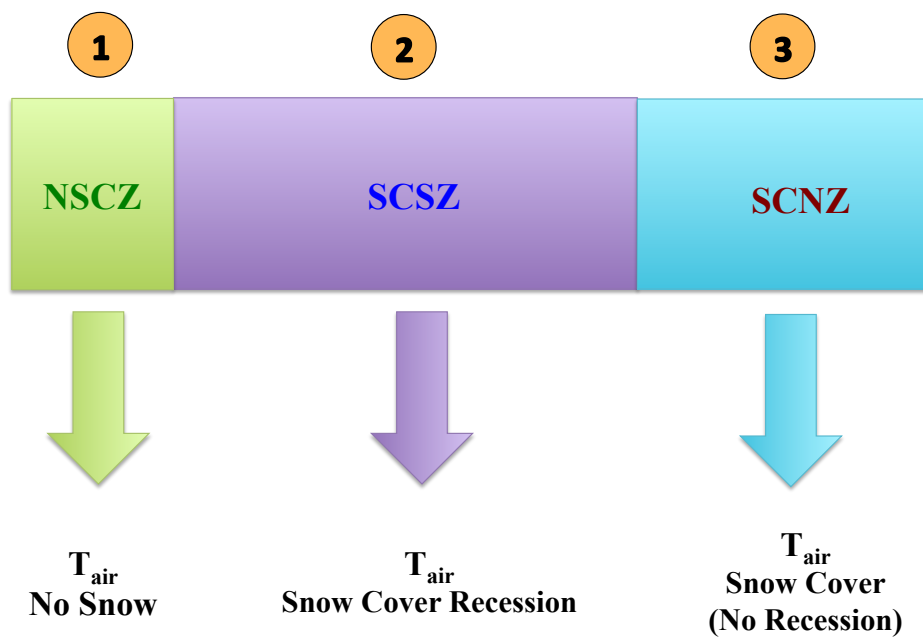
33

34



35

36 **Figure 2.** Area percentages of NSCZ, SCSZ, and SCNZ in North America and Eurasia from April through June for the period 1972-2006.



37

38 **Figure 3.** Experimental design for assessing the effects of pan-Arctic snow cover and air temperature changes on frozen soil heat content
39 (SHC) in NSCZ, SCSZ, and SCNZ over North America and Eurasia from April through June for the period 1972-2006.

40

41

42

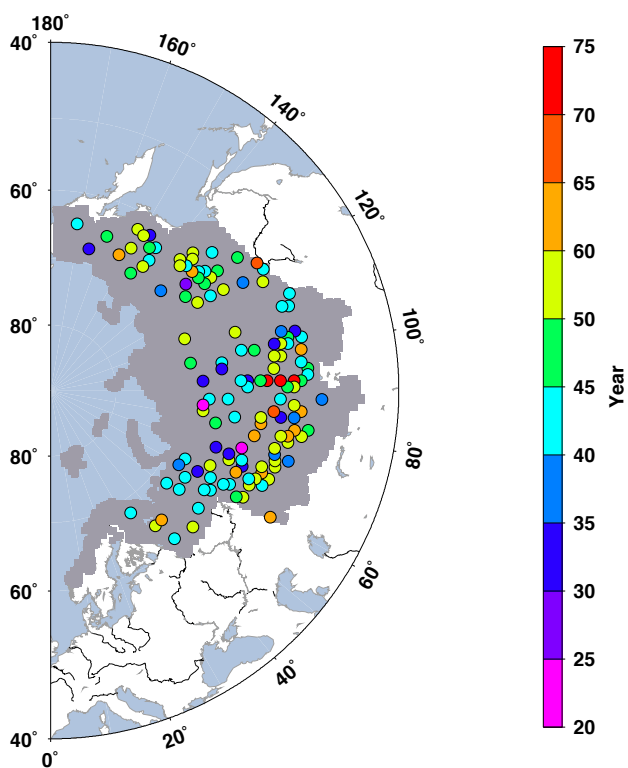
43

44



45

(a)



46

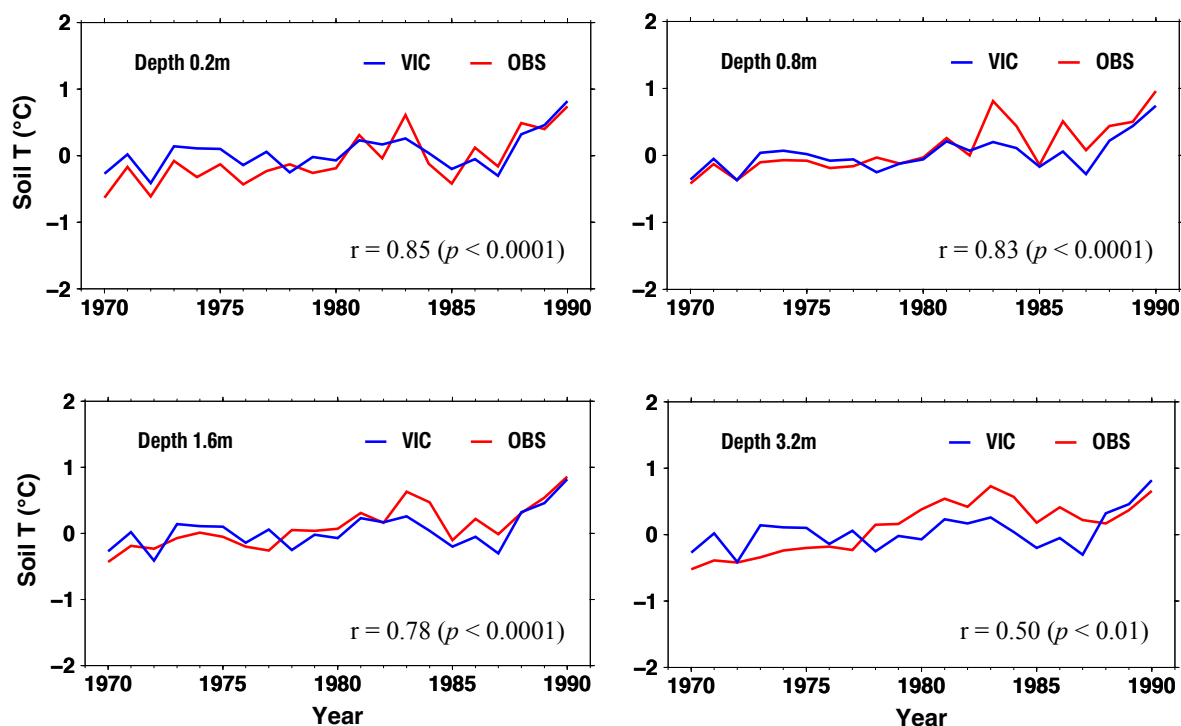
47

42



48

(b)



49

b)

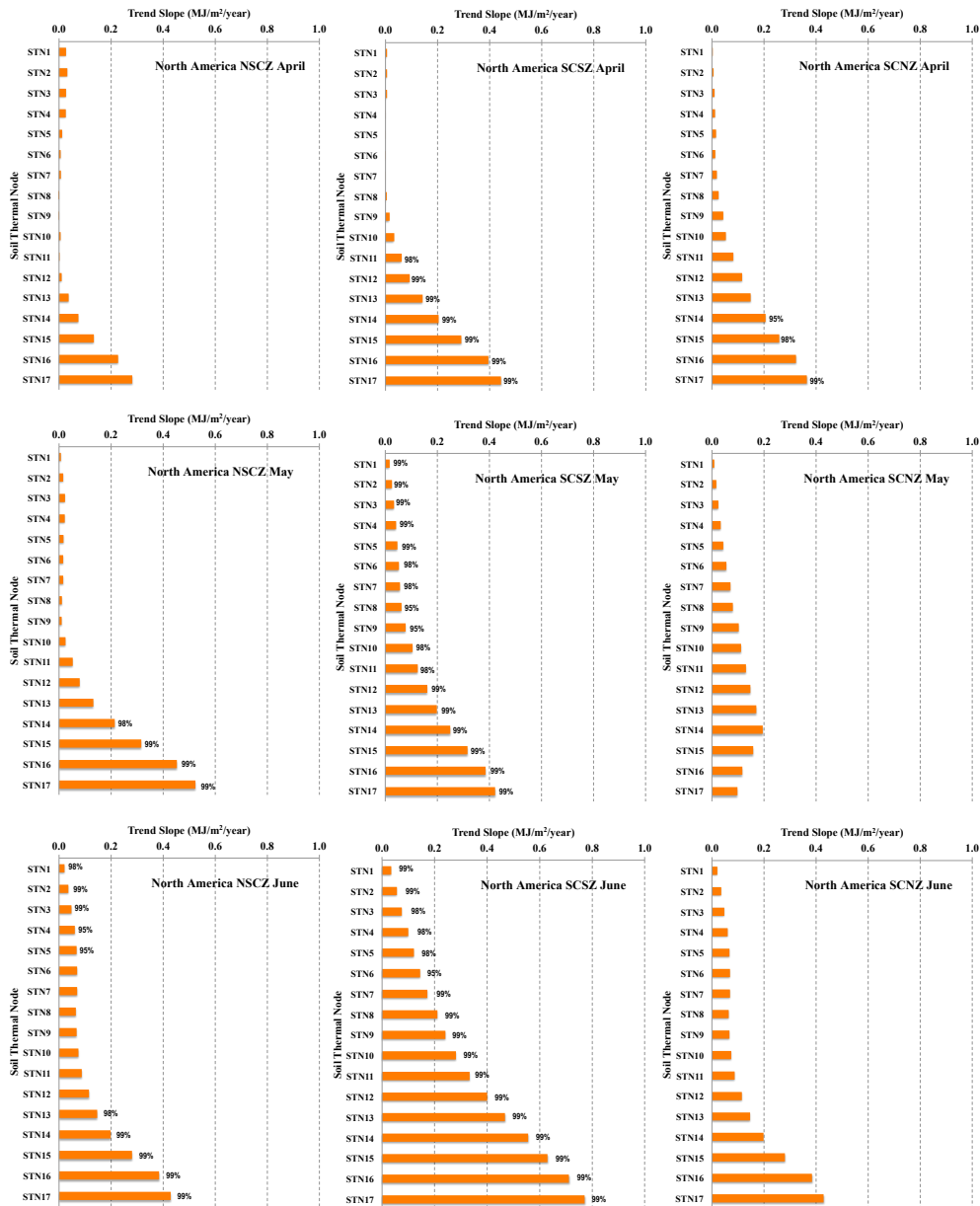
50 **Figure 4.** (a) Geographical distribution of 146 observation sites for soil temperature across the former Soviet Union. The color bar at
 51 right indicates the number of archived years of data ending in 1990. (b) Comparisons between observed and modeled soil temperature
 52 anomalies averaged over 146 observation sites across the former Soviet Union for the period of 1970-1990 at the depths of 0.2 m, 0.8 m, 1.6 m,
 53 and 3.2 m, respectively. The correlation is statistically significant at a level of $p < 0.025$.

54



755

(a)



756

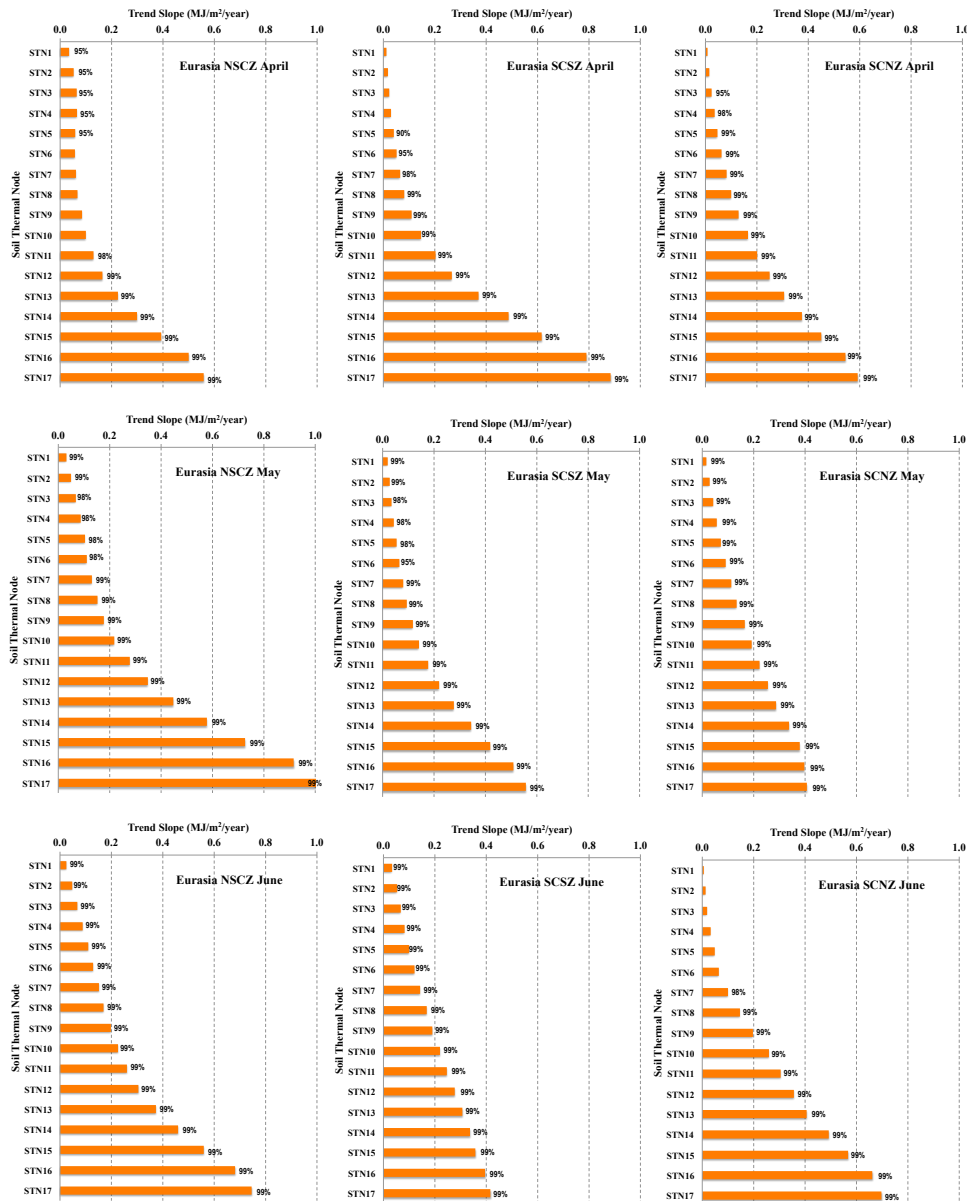
757

758

759



(b)



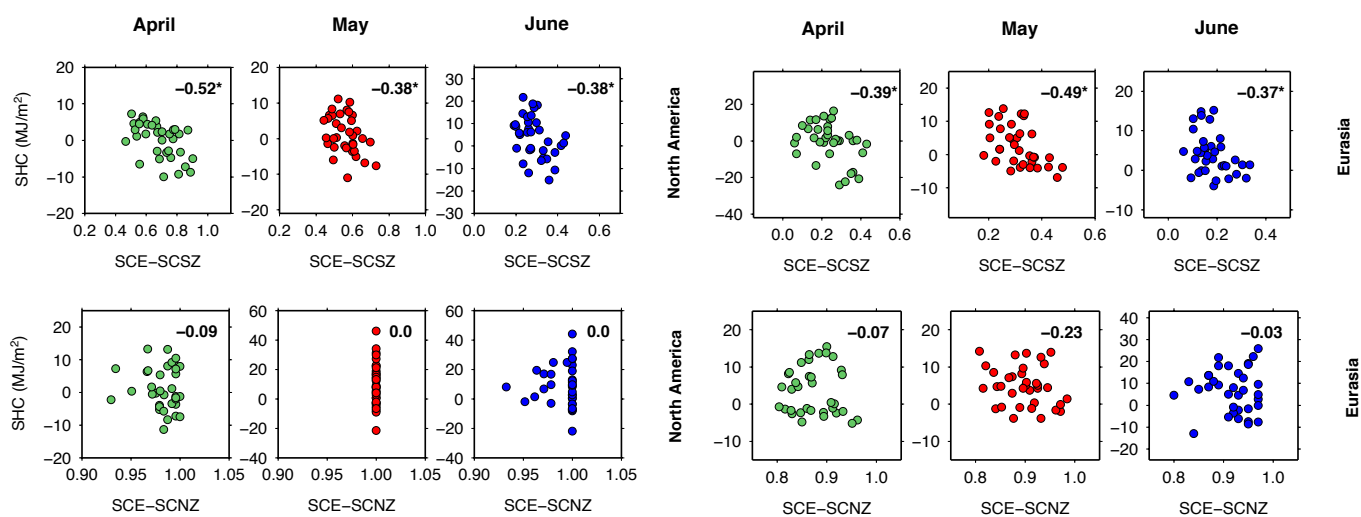
760

761 **Figure 5.** Trend analyses for SHC at the depth of each soil thermal node derived from the VIC model in
 762 NSCZ, SCSZ, and SCNZ over (a) North America and (b) Eurasia from April through June for the period
 763 1972-2006. The significance level (expressed as a confidence level) was calculated using a two-sided
 764 Mann-Kendall trend test. Trend slope units are $\text{MJm}^{-2} \text{year}^{-1}$.

765



66



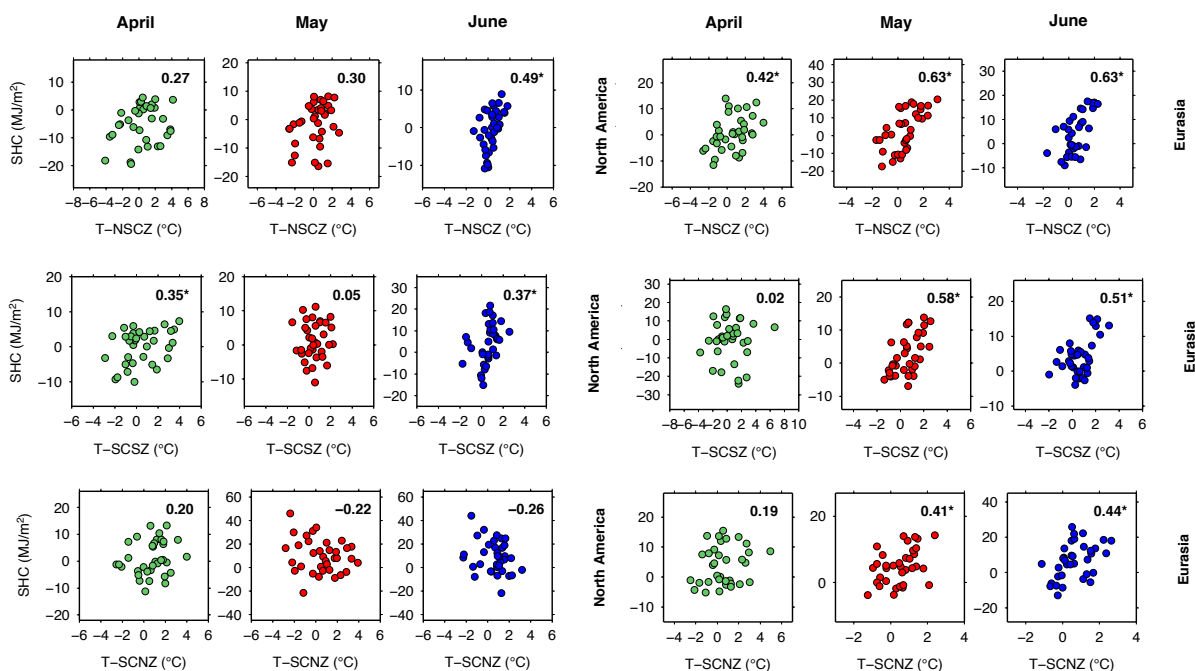
67

68 **Figure 6.** Correlations between observed SCE and simulated SHC in SCSZ and SCNZ over North America and Eurasia from April through
 69 June for the period 1972-2006. The correlation with asterisks is statistically significant at a level of $p < 0.025$ when its absolute value is greater
 70 than 0.34.

71



72



73

74 **Figure 7.** Correlations between observed SAT and simulated SHC in NSCZ, SCSZ and SCNZ over North America and Eurasia from April
 75 through June for the period 1972-2006. The correlation with asterisks is statistically significant at a level of $p < 0.025$ when its absolute value
 76 is greater than 0.34.

77



778

779 **List of Tables**

780 **Table 1.** Eighteen soil thermal nodes (STN) and their corresponding depth (m) from the
781 surface. Along the soil profile from the top to the bottom, the first STN was named as STN0
782 with a depth of 0 m indicating it is at the surface, while the deepest one is STN17 with a soil
783 depth of 15 m. The SHC for STN17 represents an averaged thermal value for the soil profile.

784 **Table 2.** Trend analyses for observed snow cover extent (SCE) in the snow covered
785 sensitivity zone (SCSZ) and the snow covered non-sensitivity zone (SCNZ) over North
786 America and Eurasia from April through June for the period 1972-2006. The significance
787 level (p -value) was calculated using a two-sided Mann-Kendall trend test. Trend slope (ts)
788 units are year⁻¹.

789

790 **Table 3.** Trend analyses for CRU monthly surface air temperature (SAT) in the non-snow
791 covered zone (NSCZ), SCSZ, and SCNZ over North America and Eurasia from April through
792 June for the period 1972-2006. The significance level (p -value) was calculated using a two-
793 sided Mann-Kendall trend test. Ts units are °Cyear⁻¹.

794

795 **Table 4.** Correlation coefficients due to the linear trend and variability for SHC derived from
796 VIC and NOAA SCE observations in SCSZ and SCNZ over North America and Eurasia from
797 April to June for the period 1972-2006. The significance level (p -value) was calculated using
798 a two-tailed Student t-test with 33 degrees of freedom.

799 **Table 5.** Correlation coefficients due to the linear trend and variability for SHC derived from
800 VIC and CRU SAT in NSCZ, SCSZ, and SCNZ over North America and Eurasia from April



801 to June for the period 1972-2006. The significance level (p -value) was calculated using a two-
802 tailed Student t-test with 33 degrees of freedom.



803

804 **Table 1.** Eighteen soil thermal nodes (STN) and their corresponding depth (m) from the
805 surface. Along the soil profile from the top to the bottom, the first STN was named as STN0
806 with a depth of 0 m indicating it is at the surface, while the deepest one is STN17 with a soil
807 depth of 15 m. The SHC for STN17 represents an averaged thermal value for the soil profile.

Soil Thermal Node	Depth (m)
STN0	0.0
STN1	0.2
STN2	0.4
STN3	0.6
STN4	0.9
STN5	1.3
STN6	1.7
STN7	2.1
STN8	2.7
STN9	3.3
STN10	4.1
STN11	5.1
STN12	6.1
STN13	7.3
STN14	8.8
STN15	10.6
STN16	12.6
STN17	15.0

808



809

810 **Table 2.** Trend analyses for observed snow cover extent (SCE) in the snow covered sensitivity zone (SCSZ) and the snow covered
 811 non-sensitivity zone (SCNZ) over North America and Eurasia from April through June for the period 1972-2006. The significance
 812 level (p -value) was calculated using a two-sided Mann-Kendall trend test. Trend slope (ts) units are year⁻¹.

813

	North America						Eurasia					
	April		May		June		April		May		June	
	$p <$	ts	$p <$	Ts	$p <$	ts	$p <$	ts	$p <$	ts	$p <$	ts
SCE-SCSZ	0.025	-0.0052	0.01	-0.0026	0.01	-0.0029	0.025	-0.0042	0.01	-0.0035	0.005	-0.0034
SCE-SCNZ	--	-0.0002	--	-0.0000	--	-0.0000	--	0.0003	--	-0.0010	--	-0.0006



14

15 **Table 3.** Trend analyses for CRU monthly surface air temperature (SAT) in the non-snow covered zone (NSCZ), SCSZ, and SCNZ over North
 16 America and Eurasia from April through June for the period 1972-2006. The significance level (p -value) was calculated using a two-sided
 17 Mann-Kendall trend test. Ts units are $^{\circ}\text{Cyear}^{-1}$.

18

	North America						Eurasia					
	April		May		June		April		May		June	
	$p <$	ts	$p <$	Ts	$p <$	ts	$p <$	ts	$p <$	ts	$p <$	ts
SAT-NSCZ	--	0.0345	--	-0.0243	0.005	0.0323	--	0.0531	0.005	0.0663	0.005	0.0412
SAT-SCSZ	--	0.0400	--	0.0243	0.005	0.0415	--	0.0143	0.005	0.0500	0.005	0.0552
SAT-SCNZ	0.005	0.0657	0.005	0.0806	0.01	0.0467	--	0.0044	0.005	0.0435	0.005	0.0471



19

20 **Table 4.** Correlation coefficients due to the linear trend and variability for SHC derived from VIC and NOAA SCE observations in SCSZ and
 21 SCNZ over North America and Eurasia from April to June for the period 1972-2006. The significance level (p -value) was calculated using a
 22 two-tailed Student t-test with 33 degrees of freedom.

			April		May		June	
			$p <$	r	$p <$	r	$p <$	r
Correlation (Trend)	North America	SCSZ	0.025	-0.9	0.025	-0.7	0.025	-0.8
		SCNZ	0.025	-0.5	--	0.0	--	0.0
	Eurasia	SCSZ	0.025	-0.9	0.025	-1.0	0.025	-0.8
		SCNZ	0.025	0.9	0.025	-0.7	0.025	-0.7
Correlation (Variability)	North America	SCSZ	--	-0.2	--	-0.1	--	0.0
		SCNZ	--	0.0	--	0.0	--	0.0
	Eurasia	SCSZ	--	-0.0	--	-0.0	--	0.1
		SCNZ	--	-0.1	--	-0.1	--	0.1

23



824

825
 826
 827

Table 5. Correlation coefficients due to the linear trend and variability for SHC derived from VIC and CRU SAT in NSCZ, SCSZ, and SCNZ over North America and Eurasia from April to June for the period 1972-2006. The significance level (p -value) was calculated using a two-tailed Student t-test with 33 degrees of freedom.

			April		May		June	
			$p <$	r	$p <$	r	$p <$	r
Correlation (Trend)	North America	NSCZ	0.025	0.3	0.025	-0.7	0.025	0.7
		SCSZ	0.025	0.9	0.025	0.7	0.025	0.8
		SCNZ	0.025	0.5	--	0.0	--	0.0
	Eurasia	NSCZ	0.025	0.9	0.025	1.0	0.025	1.0
		SCSZ	0.025	0.9	0.025	1.0	0.025	0.8
		SCNZ	0.025	1.0	0.025	0.7	0.025	0.7
Correlation (Variability)	North America	NSCZ	--	0.2	0.025	0.4	--	0.37
		SCSZ	--	0.1	--	-0.2	--	-0.1
		SCNZ	--	-0.0	--	-0.2	--	-0.2
	Eurasia	NSCZ	--	0.2	--	0.1	--	0.2
		SCSZ	--	0.0	--	0.2	--	0.1
		SCNZ	--	0.1	--	0.1	--	0.1

828